Backstepping Control of an Autonomous Catamaran Sailboat

Helmi Abrougui
U.R Automatic Control & Marine
Robotics
Naval Academy, Tunisia
helmiabrougui@yahoo.fr

Samir Nejim
U.R Automatic Control & Marine
Robotics
Naval Academy, Tunisia
samir.nejim@centraliens.net

Abstract

Automatic control of sailing boats has continuously evolved since it allows the increase of sailing safety and the improvement of cruise speed. Hence, the main problem with sailing resides in the large heel angle and important roll motion that can be caused by strong wind. In order to overtake these risks and to ameliorate the sailboat manoeuvrability and speed, a solution is to design sailboats with two or three hulls; referred, respectively, as catamaran and trimaran. This paper presents an autopilot design for an autonomous catamaran sailing vessel. A four degree of freedom dynamic model of the vehicle is firstly described using Newton's second law and kinematic equations. Due to high nonlinearity of the mathematical dynamic model of the catamaran sailboat, a nonlinear heading controller based on backstepping method is developed to stabilize the boat heading while tracking waypoints. Finally, simulation results are carried out to show the effectiveness of the proposed approach and the behaviour of the overall system.

1 Introduction

Sailing is an efficient navigation technic that uses wind kinetic energy but little to no electric energy to navigate. Therefore, sailboats are well suited for long operations such as monitoring of maritime area, oceanographic research and Microtransat challenge (Brière, 2006). In this context, many autonomous sailboat projects have been launched throughout the world over the last decade such as the AVALON, the AROO and the FASt sailboats project (Erckens et al, 2010) (Neal, 2006) (Alves et al, 2008).

The sailboat propulsion depends on the wind speed and direction. The sail is used to create forward propulsion for the sailing vessel. Depending on the polar diagram of the sailboat, there is an optimal sail angle that gives the highest forward linear speed but it can cause an important heel angle that decreases the boat stability and safety. Hence, we need an effective control of the sail and the rudder angle to reduce the roll motion. Authors (Wille et al, 2016) developed a Linear Quadratic Regulator (LQR) for controlling the momentum created by the sail. This controller reduces the roll motion so, it increases robustness and safety. Another solution for reducing roll motion is to design catamaran sailboats. Due to its two hull the catamaran sailboat is more stable than the monohull sailboat.

Figure 1: 3D printing catamaran sailboat

Classical techniques of Lagrangian and Newtonian mechanics are the most used methods for determining the mathematical model of a catamaran sailing boat. An example of a dynamic model with six Degree of Freedom 6-DoF is presented in (Furrer, 2010) using Fossen approach (Fossen, 2002).

Several control techniques have been applied in sailing vessel. The most used regulators are the Proportional Integral Derivative PID controllers (Cruz et al, 2014) and (Ramirez, 2012). This control law is designed using Nomoto's first order model. In addition, a Mamdani type fuzzy inference systems was used by authors (Stelzer et al, 2007) to control both actuators for sail and rudder. Another fuzzy-based controller has been developed in (Gomes et al, 2015) and (Abril et al, 1997) where the rudder angle was calculated via the heading and the desired angular velocity. Xiao and Jouffroy (Xiao et al, 2014) designed a nonlinear heading controller for a 4-DoF monohull sailboat model using backstepping technics. The basic idea behind this method is to break down the design problem of the full system into a sequence of sub-problems on lower order systems, and recursively use some states as "virtual input" to obtain the intermediate control laws with the Control Lyapunov Function (CLF). The main advantage of backstepping control is the guarantee of system stability.

In this paper, due to the high nonlinearities of the developed dynamic model of the catamaran sailboat, an autopilot was designed based on backstepping approach in order to steer the vehicle towards a specific target. For a given wind direction, the sail position is defined as a direct function of the boat heading.

In the following section, a dynamic model of a sailing catamaran with four degree of freedom is described. In section III, the nonlinear heading controller was designed and tested with the developed dynamic model. Finally, some simulation results were carried out to illustrate and to evaluate the studied approach.

2   System Dynamics

The dynamic model of the catamaran sailboat presented in this paper is inspired from previous researches conducted in (Jaulin et al, 2013) and (Wille et al, 2016). One of the main contributions of this paper consists of the improvement of the dynamic model by taking into consideration the roll and the sway motion. Therefore, the resulting dynamic model has 4-DoF instead of three. This dynamic model of the sailing catamaran is derived under the following assumptions:

- The sail and the rudder are modeled as rigid foils.
- Added mass coefficients (Fossen, 2002) are modeled as constants.
- The sailboat is assumed to evolve in calm waters.

The modeled catamaran sailing boat is presented in Figure 2 and Appendix B, where the North-East-Down NED coordinate system (X, Y, Z) is treated as inertial reference frame $(n - frame)$ and the (x_b, y_b, z_b) is the body fixed frame $(b - frame)$ connected to the boat.

The latter is the reference frame attached to the sailboat. It rotates with angular velocity $W = (p \; q \; r)^T$ relative to the $(n - frame)$. Its origin is assumed to coincide with the sailboat's center of gravity G.

The sailboat linear velocity in $(b - frame)$ is $V = (u \; v \; w)^T$.

The sailboat is assumed to be rigid and 4-DoF are considered, after excluding both heaving and pitching motions $q = w = 0$. (See Figure 1)

$\boldsymbol{v} = (u \; v \; r \; p)^T$ is the velocity vector in the $(b - frame)$ and $\eta = (x \; y \; \psi \; \phi)^T$ is a vector describing, the position of the sailboat, its yaw and roll in the $(n - frame)$.
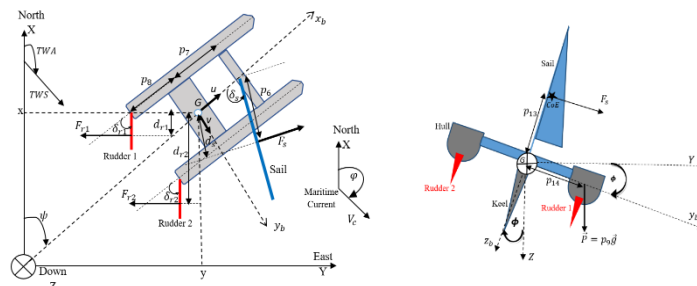

Figure 2: Top and rear view of the modelled catamaran sailboat

Vector η is then derived through a coordinate transformation (Fossen, 2002), giving the following kinematic equations of the sailboat:

$$\dot{x} = u \cos\psi - v \sin\psi \cos\phi + V_C \cos\varphi \tag{1}$$
$$\dot{y} = u \sin\psi + v \cos\psi \cos\phi + V_C \sin\varphi \tag{2}$$
$$\dot{\psi} = r \cos\phi \tag{3}$$
$$\dot{\phi} = p \tag{4}$$

Where φ and V_c are respectively the maritime current direction and speed.

The sail of the boat is inflated by the apparent wind force and consequently the sailboat advances.

According to (Xiao et al, 2014), the apparent wind AW is the vector sum of the true wind TW in $(b - frame)$ $TW^{b-frame}$ and the sailboat velocity $\boldsymbol{v}$. (Appendix A).

The true wind vector expressed in the $(n - frame)$ $TW^{n-frame}$ is given by:

$$TW^{n-frame} = \begin{pmatrix} TWS \cos TWA \\ TWS \sin TWA \\ 0 \end{pmatrix} \tag{5}$$

So,

$$TW^{b-frame} = R_2 R_1 TW^{n-frame} \tag{6}$$

With

$$R_1 = \begin{pmatrix} \cos\psi & \sin\psi & 0 \\ -\sin\psi & \cos\psi & 0 \\ 0 & 0 & 1 \end{pmatrix}$$
$$R_2 = \begin{pmatrix} 1 & 0 & 0 \\ 0 & \cos\phi & \sin\phi \\ 0 & -\sin\phi & \cos\phi \end{pmatrix}$$

Therefore, we get

$$
\begin{aligned}
AW^{b-frame} &= TW^{b-frame} - V - W \times (x_s\, y_s\, z_s)^T \\
&= \begin{pmatrix} TWS \cos(TWA - \psi) - u - r\, y_s \\ TWS \sin(TWA - \psi) \cos\phi - v - r\, x_s + p z_s \\ 0 \end{pmatrix} \\
&= \begin{pmatrix} AW^{x_b} \\ AW^{y_b} \\ 0 \end{pmatrix}
\end{aligned} \tag{7}
$$

Then

$$AWA = atan2(AW^{y_b}, AW^{x_b}) \tag{8}$$
$$AWS = \|AW^{b-frame}\|$$
$$= \sqrt{(AW^{x_b})^2 + (AW^{y_b})^2} \tag{9}$$

The angle of attack on the sail by the direction of the apparent wind AW is equal to $(\delta_s - AWA)$ (Melin, 2015). Therefore, the aerodynamic force f_s applied on the Center of Effort CoE of the sail is equal to:

$$f_s = p_4 AWS \sin(\delta_s - AWA) \tag{10}$$

The vectorial representation of this aerodynamic force in the fixed body frame $(b - frame)$ is:

$$F_s = \begin{pmatrix} f_s^{x_b} \\ f_s^{y_b} \end{pmatrix} = \begin{pmatrix} f_s \sin\delta_s \\ f_s \cos\delta_s \end{pmatrix} \tag{11}$$

On the other hand, the angle of attack on the rudders by the apparent water velocity is equal to δ_r (Melin, 2015). By assuming that the apparent water and the sailboat speeds are equal, the water generates a hydrodynamic force on each rudder which is equal to:

$$\begin{cases} f_{r1} = p_5 u^2 \sin\delta_{r1} \\ f_{r2} = p_5 u^2 \sin\delta_{r2} \end{cases} \tag{12}$$

With

$$\delta_{r1} = \delta_{r2} = \delta_r \tag{13}$$

Thus, in what follows the hydrodynamic force applied on the sailboat is supposed created by one rudder situated in $(x_b - axis)$ and equal to:

$$f_r = f_{r1} + f_{r2} = 2p_5u^2\sin\delta_r \tag{14}$$

The vectorial representation of this hydrodynamic force in the fixed body frame ($b - frame$) is then

$$F_r = \begin{pmatrix} f_r^{x_b} \\ f_r^{y_b} \end{pmatrix} = \begin{pmatrix} -f_r\sin\delta_r \\ -f_r\cos\delta_r \end{pmatrix} \tag{15}$$

For simplicity reasons, the sailboat is affected by some tangential friction forces $-p_1u^2$ and $-p_2v$ respectively applied on ($x_b - axis$) and ($y_b - axis$) also it is affected by an angular friction force $-p_3r$ applied around ($z_b - axis$).

In addition, the applied forces on the sailboat are F_s and F_r. Therefore, according to Newton's second law of motion applied in the ($b - frame$) , we have:

$$(p_9 - X_{\dot{u}})\dot{u} = f_s^{x_b} + f_r^{x_b} - p_1u^2 \tag{16}$$

$$= f_s\sin\delta_s - f_r\sin\delta_r - p_1u^2$$

$$(p_9 - Y_{\dot{v}})\dot{v} = f_s^{y_b} + f_r^{y_b} - p_2v \tag{17}$$

$$= f_s\cos\delta_s - f_r\cos\delta_r - p_2v \tag{18}$$

$$(p_{10} - N_{\dot{r}})\dot{r} = d_sf_s - d_rf_r - p_3r$$

With

$$d_s = p_6 - p_7\cos\delta_s$$

$$d_r = p_8\cos\delta_r$$

By adding the Coriolis effect caused by both rigid body and added mass (Wille et al, 2016) we get:

$$(p_9 - X_{\dot{u}})\dot{u} = f_s\sin\delta_s - f_r\sin\delta_r + vr(p_9 - Y_{\dot{v}}) - p_1u^2 \tag{19}$$

$$(p_9 - Y_{\dot{v}})\dot{v} = f_s\cos\delta_s - f_r\cos\delta_r + ur(X_{\dot{u}} - p_9) - p_2v \tag{20}$$

$$(p_{10} - N_{\dot{r}})\dot{r} = (p_6 - p_7\cos\delta_s)f_s - p_8\cos\delta_r f_r + uv(Y_{\dot{v}} - X_{\dot{u}}) - p_3r \tag{21}$$

According to Le Bars (Le Bars et al, 2013) the roll motion is supposed to be pendulum:

$$\dot{p} = \frac{z_sf_s\cos\delta_s\cos\phi - p_{13}p_9g\sin\phi - p_{12}p}{p_{11} - K_{\dot{p}}} \tag{22}$$

Therefore, the 4-DoF state equations, which describe the dynamics of the sailboat, are:

$$\begin{cases} \dot{x} = u\cos\psi - v\sin\psi\cos\phi + V_C\cos\varphi \\ \dot{y} = u\sin\psi + v\cos\psi\cos\phi + V_C\sin\varphi \\ \dot{\psi} = r\cos\phi \\ \dot{\phi} = p \\ \dot{u} = \dfrac{(f_s\sin\delta_s - f_r\sin\delta_r + vr(p_9 - Y_{\dot{v}}) - p_1u^2)}{(p_9 - X_{\dot{u}})} \\ \dot{v} = \dfrac{(f_s\cos\delta_s - f_r\cos\delta_r + ur(X_{\dot{u}} - p_9) - p_2v)}{(p_9 - Y_{\dot{v}})} \\ \dot{r} = \dfrac{((p_6 - p_7\cos\delta_s)f_s - p_8 f_r\cos\delta_r + uv(Y_{\dot{v}} - X_{\dot{u}}) - p_3r)}{(p_{10} - N_{\dot{r}})} \\ \dot{p} = \dfrac{z_sf_s\cos\delta_s\cos\phi - p_{13}p_9g\sin\phi - p_{12}p}{p_{11} - K_{\dot{p}}} \end{cases} \tag{23}$$

This system state space (23) is highly nonlinear and it has the following compact notation; $\dot{X} = f(X, U, B)$
With:

$X = (x\ y\ \psi\ \phi\ u\ v\ r\ p)^T$ the state vector.

$U = \begin{pmatrix} \delta_s \\ \delta_r \end{pmatrix}$ the input vector.

B, disturbance due to maritime current.

The two actuators, sail and rudder, have physical limitations. In this dynamic model, these limitations are expressed by setting the maximum sail opening angle to $\delta_s^{max} = 90°$ and the maximum angular velocity to 30 fl/s. In (Santos et al, 2016) and (Xiao et al, 2014), the control of the sail opening angle was assured by setting

the length of the rope which is attached to the boom. However, in this paper, it is assumed that the sail is rotated by a servomotor built in the mast. Therefore, the sail and servo angle were assumed to be equal.

The rudder will follow similar limitations, $\delta_r^{max} = 45°$ for maximum rudder angle and 30 fl/s for its maximum angular velocity.

3   Autopilot Design

To make an autonomous catamaran sailboat follow a given path or reach a target position (x_d, y_d), a controller with two levels is designed as presented in Figure 3. The first one is a high-level controller. It generates the desired heading ψ^{ref} and the sail opening angle δ_s for a sailing trip. The second controller is the autopilot. It usually sails the boat to the desired heading. In this paper, we will focus on the autopilot design. Regarding the navigation strategy (high-level controller), we will use the waypoint tracking proposed in (Jaulin, 2014) with minor improvements.
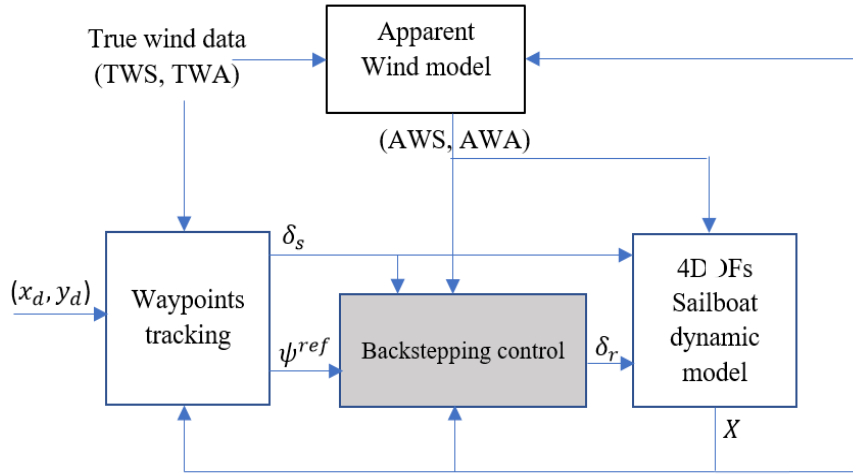
Figure 3: Proposed control scheme

3.1   Heading Control

To use the backstepping techniques we consider again the subsystem described by the two differential equations (3) and (21).

The heading error is: $e_1 = \psi^{ref} - \psi$, its dynamics is written as $\dot{e}_1 = -r \cos \phi$ since $\dot{\psi^{ref}} = 0$

Let the Control Lyapunov Function be defined as

$$V_1 = \frac{1}{2} e_1^2 \tag{24}$$

We first choose r as the virtual control input to converge the system toward $e_1 = 0$ with a stabilizing function $g_1(e_1, \phi)$ such that $\dot{V}_1 < 0$ for all $e_1 \neq 0$.

We have
$$\dot{V}_1 = e_1 \dot{e}_1 = -r e_1 \cos \phi \tag{25}$$

By taking $r = g_1(e_1, \phi) = \frac{k_1 e_1}{\cos \phi}$ we obtain $\dot{V}_1 = -k_1 e_1^2 < 0$

Where k_1 is a positive design constant.

However, since r is not the system input, we can achieve $r = g_1(e_1, \phi) = \frac{k_1 e_1}{\cos \phi}$ only with an error that is represented by the new variable error

$$e_2 = g_1(e_1, \phi) - r \tag{26}$$

The new dynamic errors are:

$$\begin{cases} \dot{e}_1 = -r\cos\phi = \cos\phi\left(e_2 - \frac{k_1 e_1}{\cos\phi}\right) = e_2\cos\phi - k_1 e_1 \\ \dot{e}_2 = \frac{k_1}{\cos^2\phi}(e_1 p\sin\phi - r\cos^2\phi) - h(\psi, r, u, v, \delta_r, f_s) \end{cases} \quad (27)$$

with

$$h(\psi, r, u, v, \delta_r, f_s) = \dot{r} \quad (28)$$

So, the new control Lyapunov function V_2 can be written as

$$V_2 = \frac{1}{2}e_1^2 + \frac{1}{2}e_2^2 \quad (29)$$

Then

$$\dot{V}_2 = e_1\dot{e}_1 + e_2\dot{e}_2 \quad (30)$$

given that

$$e_1\dot{e}_1 = e_1(e_2\cos\phi - k_1 e_1) \quad (31)$$

$$e_2\dot{e}_2 = e_2\left(\frac{k_1}{\cos^2\phi}(-r\cos^2\phi + e_1 p\sin\phi) - h(\psi, r, u, v, \delta_r, f_s)\right) \quad (32)$$

$\dot{V}_2$ can be rewritten as:

$$\dot{V}_2 = e_1 e_2\cos\phi - k_1 e_1^2 - e_2 h(\psi, r, u, v, \delta_r, f_s) - e_2 k_1 r + \frac{e_2 e_1 k_1 p}{\cos^2\phi}\sin\phi \quad (33)$$

By choosing

$$h(\psi, r, u, v, \delta_r, f_s) = e_1\left(cos\,\phi + \frac{k_1 k_2}{cos\,\phi} + \frac{k_1 p\,sin\,\phi}{\cos^2\phi}\right) - r(k_1 + k_2) \quad (34)$$

We get

$$\dot{V}_2 = -k_1 e_1^2 - k_2 e_2^2 < 0 \quad \forall \quad e_1 \neq 0, \ e_2 \neq 0 \quad (35)$$

With $k_2 \in \Re^{*+}$
Using equations (14), (28) and (34) we obtain:

$$\delta_r = 0.5\,sin^{-1}\left(\frac{(p_6 - p_7\,cos(\delta_s))f_s + uv(Y_{\dot{v}} - X_{\dot{u}}) - r(p_3 - (p_{10} - N_{\dot{r}})(k_1 + k_2)) - e_1(p_{10} - N_{\dot{r}})\left(cos\,\phi + \frac{k_1 k_2}{cos\,\phi} + k_1 p\frac{sin\,\phi}{\cos^2\phi}\right)}{0.5 p_5 p_8 u^2}\right) \quad (36)$$

With

$$\begin{cases} \delta_r < |\delta_r^{max}| \\ u \neq 0 \quad \forall \ X \in \Re^8 \end{cases}$$

3.2 Navigation Strategy

Based on the polar diagram[1] given in Figure 5 and using the target position (x_d, y_d), the system state space and the wind direction, the high-level controller which is inspired from (Jaulin, 2014) generates the desired heading ψ^{ref} and the sail opening angle δ_s.

As we know, a sailing boat cannot sail directly against the wind direction because in this case the sail will be luffing in the breeze and cannot generate any propulsive power.

The polar diagram (see Figure 5) shows the sector of directions that cannot be navigable by sailboats. It is called a no-go-zone. The size of the no-go zone, referred to as the no-go-heading, will differ based on characteristics of the particular sailboat.

To avoid this no-go-zone, the boat has to sail in Zig-Zag course and execute tack[2] manoeuver so, the high-level controller must generate desired heading $\psi^{ref} \notin \,]\text{TWA} + \pi - \xi, \text{TWA} - \pi + \xi[$.

---

[1] is the set of all pairs (ψ, u) that can be reached by the sailboat when it navigates.
[2] The sailboat tacks, that is sails on alternating sides of the wind and therefore advances towards the wind. This is the most complex case, testing the interaction between all parts of the model, especially rudder and sail forces.

So, in the case where the sailboat has to navigate with maximum speed on an upwind navigation ($TWA = \pi + \psi$) the following set of headings are used.

$$\psi_1^{ref} = TWA + \pi - \xi - \beta \quad \text{and} \quad \psi_2^{ref} = TWA - \pi + \xi + \beta \tag{37}$$

For downwind sailing, the desired heading given by the high-level controller is defined by the following $atan2$ function[3]:

$$\psi_3^{ref} = atan2(y - y_d, x - x_d) \tag{38}$$

which allows the sailboat to navigate directly toward its destination.

Using the algorithm given in (Santos, 2016) and presented on Figure 4, the overall system was simulated to evaluate the control law developed in this work.

In what follows, the wind is simulated coming from the North ($TWA = -\frac{\pi}{2}$) and its speed is equal to 10 m/s.

Therefore the sail opening angle is given by the following equation, it depends on the sailboat heading ψ:

$$\delta_s = \pi \left[\frac{\psi}{2\pi} + \frac{1}{4} \right] + \frac{\pi}{4} - \frac{\psi}{2} \tag{39}$$

Using equations (27) and (34) the error dynamics is

$$\begin{cases} \dot{e}_1 = e_2 \cos\phi - k_1 e_1 \\ \dot{e}_2 = -e_1 \left(\cos\phi + \dfrac{k_1 k_2}{\cos\phi} \right) + r k_2 \end{cases} \tag{40}$$

Hence, the controller (36) is tuned with $k_1 = k_2 = 1$ using the pole placement method applied to equation system (40).
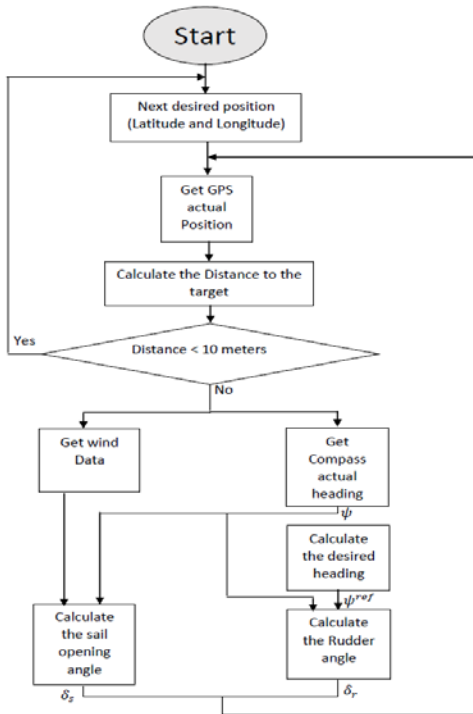

Figure 4: Algorithm used to control the sailboat
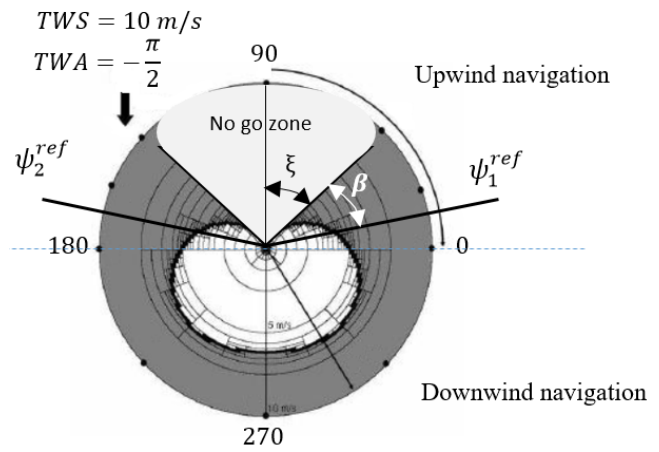(Guidance, Navigation and Control)

Figure 5: Sailboat polar diagram
$\xi = \frac{\pi}{4}$, $\beta = \frac{\pi}{12}$

---

[3] $atan2(y, x) \in [-\pi, \pi]$ is the four-quadrant inverse tangent.

4   Simulation and Results

Four set of simulations have been studied in order to show the path followed by the sailboat against the wind direction. In these simulations, the target is situated in position $(x_d = 0 ; y_d = 0)$. The simulations started with initial values $X(t = 0) = (x_i\ y_i\ \psi_i\ 0\ 8\ 0\ 0\ 0)^T$ with $i \in \{1,2,3,4\}$ and stopped when the target position was reached with a distance equal to ten meters.

The proposed control law allows the sailboat to reach the target position. Figure 6 clearly shows that the boat sails on Zig-Zag course when the target is situated against the true wind direction $i \in \{3,4\}$. However, it goes directly to the target position in downwind case $i \in \{1,2\}$. We can conclude that there is a good synchronization between the sail opening angle Figure 8 and the rudder control Figure 7 in order to execute the upwind tack maneuver. Figure 9 shows that the heading $\psi(t)$ eventually converges to the desired heading $\psi^{ref}(t)$ with an error $\psi^{ref}(t) - \psi(t) = 0$.
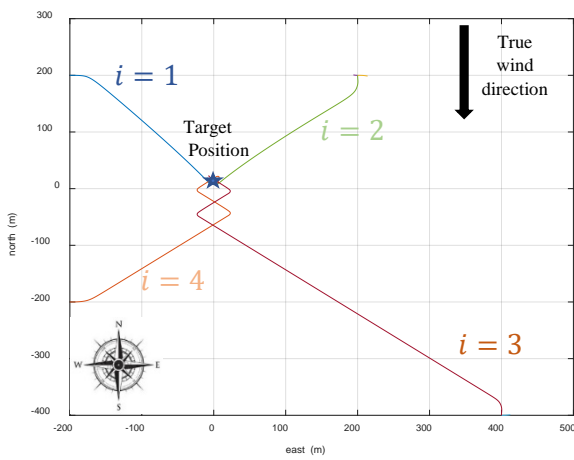

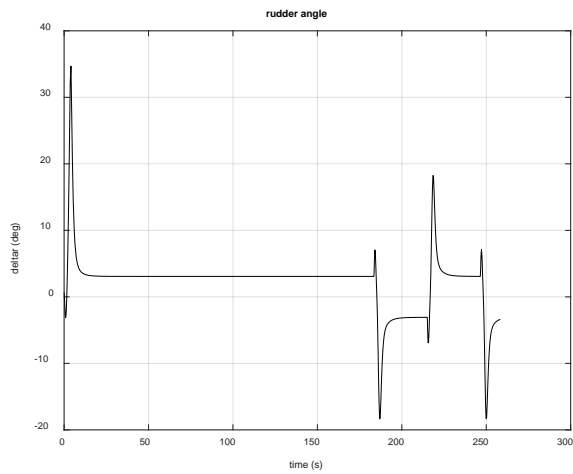Figure 6: Paths followed by the catamaran sailboat
$(x_d = 0 , y_d = 0)$

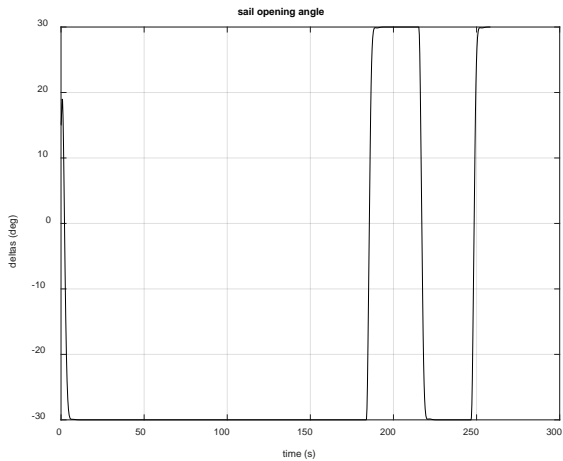Figure 7: Time evolution of the rudder angle control $(i = 3)$

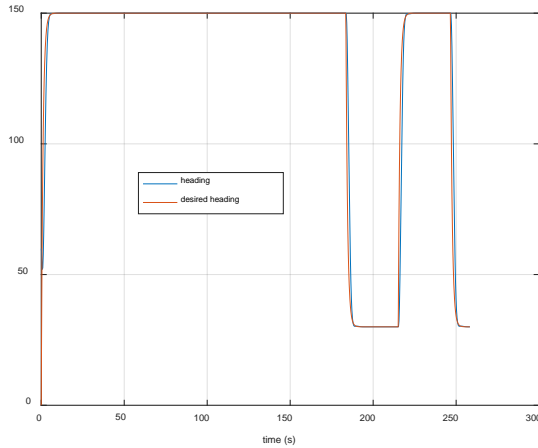Figure 8: Time evolution of the sail opening angle $(i = 3)$

Figure 9: Time evolution of the desired heading ψ^{ref} and the sailboat heading ψ $(i = 3)$

5 Conclusion

In this paper, a 4-DoF mathematical model describing the dynamic motion of a catamaran sailboat was presented. This dynamic model is considered a satisfactory model to represent the vehicle dynamic motion in the horizontal plane. The backstepping control method is used to develop a nonlinear heading control for the sailing boat. This controller works as intended. It allows to keep the sailboat on a predefined heading while waypoint tracking. The control system stability was proved using Control Lyapunov Function. As a future work in this area, it is suggested to identify the considered 3D printed catamaran sailboat (Figure 1) model parameters using the temporal variation data of the yaw angle (Casado et al, 2005). Afterwards, the implementation of the developed control law in real time will be done.

References

Cruz, N. A., & Alves, J. C. (2014). Navigation performance of an autonomous sailing robot. *In Oceans-St. John's*, (pp. 1-7). *IEEE*.

Erckens, H., Büsser, G. A., Pradalier, C., & Siegwart, R. Y. (2010). Navigation strategy and trajectory following controller for an autonomous sailing vessel. *IEEE RAM*, 17, 47-54.

Jaulin, L., & Le Bars, F. (2013). A simple controller for line following of sailboats. *In Robotic Sailing* (pp. 117-129). *Springer, Berlin, Heidelberg*.

Jaulin, L. (2004). Modelisation et commande d'un bateau à voile. In *Proceedings of 3rd Conference Internationale Francophone d'Automatique, Douz, Tunisie*.

Furrer, F. (2010). Developing a simulation model of a catamaran using the concept of hydrofoils. *ETH, Zurich*.

Romero-Ramirez, M. A. (2012). Contribution à la commande de voiliers robotisés (*Doctoral dissertation, Paris 6*).

Stelzer, R., Proll, T., & John, R. I. (2007). Fuzzy logic control system for autonomous sailboats. *In Fuzzy Systems Conference*, 2007. *FUZZ-IEEE. IEEE International* (pp. 1-6).

Xiao, L., & Jouffroy, J. (2014). Modeling and nonlinear heading control of sailing yachts. *IEEE Journal of Oceanic engineering*, 39(2), 256-268.

Gomes, L., Santos, M., Pereira, T., & Costa, A. (2015). Model-based development of an autonomous sailing Yacht controller. *In Autonomous Robot Systems and Competitions* (ICARSC), *IEEE International Conference on* (pp. 103-108). IEEE

Wille, K. L., Hassani, V., & Sprenger, F. (2016). Roll stabilization control of sailboats. *IFAC-Papers OnLine*, 49(23), 552-556.

Santos, D., Silva Junior, A. G., Negreiros, A., Vilas Boas, J., Alvarez, J., Araujo, A., & Gonçalves, L. M. (2016). Design and implementation of a control system for a sailboat robot. *Robotics*, 5(1), 5.

Casado, M. H., & Ferreiro, R. (2005). Identification of the nonlinear ship model parameters based on the turning test trial and the backstepping procedure. *Ocean Engineering*, 32(11-12), 1350-1369.

Wille, K. L., Hassani, V., & Sprenger, F. (2016). Modeling and Course Control of Sailboats. *IFAC-PapersOnLine*, 49(23), 532-539.

Le Bars, F., Jaulin, L., & Ménage, O. (2013). Suivi de ligne pour un voilier: application au robot voilier autonome VAIMOS pour l'océanographie. *In Journées des Démonstrateurs* (p. xx).

Fossen, T. I. (2002). Marine Control System-Guidance, Navigation and Control of Ships, Rigs and Underwater Vehicles. *Marine Cybemetics*.

Neal, M. (2006). A hardware proof of concept of a sailing robot for ocean observation. *IEEE Journal of Oceanic Engineering*, 31(2), 462-469.

Alves, J. C., & Cruz, N. A. (2008). Fast-an autonomous sailing platform for oceanographic missions. *In OCEANS* (pp. 1-7). *IEEE.*

Melin, J. (2015). Modeling, control and state-estimation for an autonomous sailboat.

Brière, Y. (2006). The first microtransat challenge. *Google Scholar.*

Abril, J., Salom, J., & Calvo, O. (1997). Fuzzy control of a sailboat. *International Journal of Approximate Reasoning*, 16(3-4), 359-375.

Appendix A. Wind velocity representation
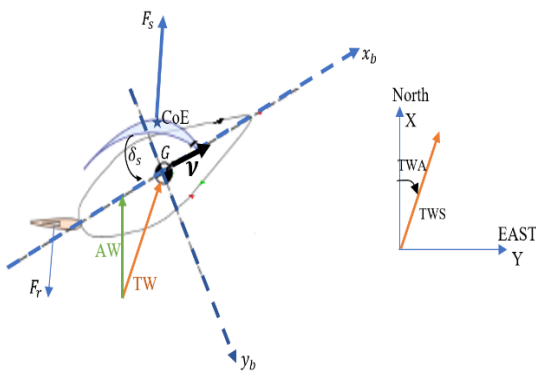
Appendix B. Variable description

Notation	Description
TW, AW	-true and apparent wind vector.
TWS, TWA	-true wind speed and direction.
AWS, AWA	-apparent wind speed and direction
V_C, φ	-maritime current speed and direction
(x, y)	-north east position
(x_s, y_s, z_s)	-coordinate of the CoE of the sailboat in (b-frame).
ψ, ϕ	-yaw and roll angle in the (n-frame).
δ_s	-sail opening angle in the (b-frame).
δ_{r1}, δ_{r2}	-rudder angle in the (b-frame).
u, v	-surge and sway motion in the (b-frame).
r, p	-angular velocity in yaw and roll (b-frame).
f_s	-aerodynamic force of the wind applied on the sail
f_{r1}, f_{r2}	-hydrodynamic forces of the water applied on the left and right rudder in the (b-frame).
g	-gravity.
p_1, p_2	-water friction in (x_b_axis) and (y_b_axis).
p_3	-water angular friction.
p_4, p_5	-lift coefficient of the sail/rudder.
p_6	-distance between the mast and CoE.
p_7	-distance between the boat's center of gravity and the mast.
p_8	-distance between G and the rudder.
p_9	-total mass of the boat.
p_{10}, p_{11}	-moment of inertia Z-axis / X-axis.
p_{12}	-roll friction coefficient.
p_{13}	-length of the equivalent pendulum in roll motion (in m).
ξ	-width of the no-go-zone, this parameter depends on the sailboat characteristics.
β	-an angle which gives maximum speed when the sailboat is on an upwind navigation.
$X_{\dot{u}}, Y_{\dot{v}}, N_{\dot{r}}, K_{\dot{p}}$	-added mass in (b-frame)